Tradeoffs among hydrodynamics, sediment fluxes and vegetation community in the Virginia Coast Reserve, USA

William Nardin[1], Laurel Larsen[2], Sergio Fagherazzi[3] and Patricia Wiberg[4]

[1] Horn point laboratory, University of Maryland Center for Environmental Science, Cambridge, MD USA

[2] Department of Geography, University of California - Berkeley, Berkeley, CA USA

[3] Department of Earth Sciences, Boston University, Boston, MA USA

[4] Department of Environmental Sciences, University of Virginia, Charlottesville, VA USA

Abstract

Both submerged and emergent vegetation plays a fundamental role in coastal bays. Vegetation stabilizes the substrate, increasing resilience to storms. Vegetation also traps sediments favoring accretion and therefore counteracting sea level rise. Previous modeling studies on flow-vegetation-sediment interactions have focused on one specific vegetated community, but we lack a general understanding of the synergistic effects of multiple vegetation species. We focus our study on the Virginia Coast Reserve Long Term Ecological Research (LTER) site, USA, where we apply numerical modeling (Delft3D-SWAN) to investigate the independent and synergistic effects of salt marsh vegetation and seagrass. Our numerical results show that salt marshes and seagrass beds reduce the volume of water entering and exiting the shallow coastal bays up to 15% during each tidal cycle. Vegetation also reduces bed shear stress and hence increases sediment deposition in the bay and marshes up to 10% compared to the no-vegetated case. Our study shows the double benefits of seagrass as an ally of salt marsh in promoting bays resilience. On the one hand, seagrass helps the salt marsh to survive during storms by reducing wave energy; on the other hand, seagrass generates more friction in subtidal parts of the bay where salt marsh cannot survive.

1. Introduction

Salt marsh and seagrass vegetation colonizes coastal landscapes, controlling the dynamics of the interface between land and ocean. The potential for rapid coastline change in the face of sea-level rise or other stressors is alarming. In addition to coastal erosion and submergence, nutrient- and turbidity-related water pollution is a growing concern for coastal estuaries (Hagy et al., 2004; Kemp et al., 2004). For both types of challenges — coastal erosion and water quality — loss of vegetation communities plays a cardinal role in triggering or exacerbating processes with socio-economic consequences. Loss of marsh vegetation puts coastal communities at greater risk of sea level rise-induced damages, whereas loss of seagrasses due to pollution or high turbidity impacts coastal fisheries (Kemp et al., 2005; Boesch, 2006). Both types of vegetation are involved in multiscale feedbacks with flow and sediment transport (Larsen and Harvey, 2010; Moore et al., 2004; Nardin and Edmonds, 2014; Fagherazzi et al., 2004; 2012), which make coastal ecosystems respond to perturbations in nonlinear ways that are difficult to predict. Although models have provided quantitative insight into vegetation-sediment feedbacks involving emergent marsh vegetation (Nardin et al., 2016; Temmerman et al., 2005) or seagrasses (Folmer et al., 2012; Carr et al., 2010; Newell and Koch, 2004), studies have not yet evaluated how these different communities interact in the estuarine landscapes. More generally, ecogeomorphic models typically represent vegetation as just a single set of parameters, despite the emerging empirical understanding that different sets of plant species have different roles in landform and landscape development (Gurnell et al., 2010; Marani et al., 2013). Quantifying these distinct and interactive roles of different vegetation communities will advance understanding of how coastal ecosystems respond to multiple stressors and improve planning of "soft" engineering projects designed to buffer the coastal environment against sea-level rise and

storm surges (Temmerman et al., 2013). Recently many coastal bays and estuaries have been impacted by a decline in suspended sediment concentration due to damming of upstream rivers (Dai et al., 2016). Vegetation can partly mitigate the decrease in sediment supply by promoting trapping of the available sediment.

The broad goal of this project is to distinguish the independent and synergistic effects of salt marsh vegetation and seagrass on water and sediment residence time and erosion/deposition dynamics in an estuarine landscape. We focus our effort on the coastal bays of the Virginia Coast Reserve (VCR), where we test different theories related to vegetation composition and sediment transport feedbacks on landscape evolution. The VCR is a system of microtidal shallow coastal bays (tidal range ~1.2 m), with shallow seagrass beds in portions of the system and extensive fringing salt marshes. As in many floodplains, river deltas, estuaries, and salt marshes, geomorphology is a dominant driver of ecosystem services provided by the VCR, such as reduction in storm impacts (waves and storm surge). Here and elsewhere, vegetation influences flow resistance (Luhar and Nepf, 2013), erosion (Collins et al., 2004), mineral sediment deposition (D'Alpaos et al., 2007; Nardin and Edmonds, 2014; Nardin et al., 2016), and organic sedimentation (Mudd et al., 2010). Our focus in this study is primarily on the hydrodynamic and sediment transport impacts of different vegetation communities.

In coastal wetlands such as the intertidal marshes and tidal flats of the VCR (Lawson et al., 2007; McLoughlin et al., 2015), wind waves, tides and vegetation jointly control water fluxes and redistribution of sediments (Cucco and Umgiesser, 2006). An assessment of water circulation patterns based on hydrodynamic models forced by realistic ocean conditions is essential. Accordingly, a two-dimensional depth averaged (2-DH) hydro-morphodynamic model that computes the flow field and sediment transport is necessary for accurately estimating water

fluxes and sediment concentration. We use the hydrodynamic model Delft3D (Lesser et al., 2004) coupled to the wave model SWAN (Booij et al., 1999) to determine the high-resolution distribution of tidal currents and waves necessary for our study. As a step toward evaluating the feedbacks between different species of vegetation and sediment deposition in shallow coastal bay systems, we ran the model for several spatial configurations of vegetation, in which seagrass and emergent marsh grasses are specified with different sets of parameters using the vegetation schematization of Baptist et al., (2005). Our work extends beyond other 2D modeling studies of this area, which focused only on the hydrodynamics or sediment resuspension in the bays in the absence of vegetation to constrain the amount of data (Fugate et al., 2006; Lawson et al., 2007; Mariotti et al., 2010; Safak et al., 2015; Wiberg et al., 2015). To assess the impacts of overwash deposition on back barrier marsh morphology, other studies focused on the interaction between barrier islands and only one species of back barrier vegetation in specific parts of the bay (Oertel et al., 2001; Walters et al. 2014), rather than in the whole system. Our goal is to explore the effects of salt marsh and seagrass on sediment transport with emphasis on erosion and deposition patterns in the VCR. Previous modeling attempts did not investigate the interactions between multiple vegetation species. Our approach quantifies the impact on the hydrodynamic and sediment transport of each single vegetation species (salt marsh and seagrass) and then the synergetic presence.

2. Methods and model set up

2.1 Study Area – The Virginia Coast Reserve

The VCR is a system of barrier islands, shallow bays, and salt marshes located on the southern part of the Delmarva Peninsula, along the U.S. mid-Atlantic coast (Fig. 1). The bays of the VCR, like many others on the eastern U.S. seaboard, lack any significant fluvial source of

freshwater and sediments. Shallow flats dominate the bays, with depths averaging 1 m below mean sea level. A network of tidal channels (5 m deep on average but exceeding 10 m at the inlets) connects the bays to the Atlantic Ocean. Emergent saltmarsh cordgrass (*Spartina alterniflora*) forms fringing low marshes around the bays, while submerged eelgrass (*Zostera marina*) occupies a portion of subtidal areas shallower than a mean depth of 1.6 m (Fig. 2). Because the study site has experienced little direct human impact, it is an ideal natural laboratory to study bay evolution and salt marsh processes (McGlathery et al., 2007).

The Delmarva Peninsula is one of areas most affected by sea level rise on the U.S. Atlantic coast (Emory and Aubrey 1991; Sallenger et al. 2012), with a relative sea level rise rate of 4 mm/year. The tide in the VCR is semidiurnal with a mean tidal range of about 1.2 m. Winds are a dominant forcing on circulation, with an annual average direction from the S-SSW and episodic northeasterly storms.

Collectively, wind waves, storm-induced currents, and tides constitute major controls on the spatial distribution of sediment resuspension within the bays (Lawson et al. 2007; Wiberg et al. 2015); while vegetation plays an important role on sediment deposition (D'Alpaos et al., 2007). In the 1930s, the bays of the VCR changed from a highly productive seagrass dominated system to an algae-dominated system (McGlathery et al., 2001), but recent restoration activities have re-planted seagrass (Orth et al., 2012; McGlathery et al., 2012), with seagrass meadows currently occupying 25 km^2 of the bays.

2.2 Model description

Delft3D-SWAN couples the computation of hydrodynamics with sediment transport and vegetation. Here, a water and sediment mass balance is carried out in two dimensions throughout the entire modeled system, and alternate realizations are run to determine how different

vegetation configurations (Fig. 3) affect residence times and sediment deposition. The flow resistance effects of vegetation are implemented through depth integrated computations, formulated in accordance with the equations proposed by Baptist (2005) (see section 2.3). Fluid flow, sediment transport, and morphological evolution are resolved in a coupled fashion. Defining a three-dimensional system with the *x, y* and *z* -axis for respectively, longitudinal, transversal, and vertical upward coordinate, the shallow water equations governing fluid flow is:

$$\frac{\partial U}{\partial t} + U\frac{\partial U}{\partial x} + V\frac{\partial U}{\partial y} = -g\frac{\partial \eta}{\partial x} + g\frac{U\left(U^2+V^2\right)^{1/2}}{C_b h} + \frac{\partial}{\partial x}\left(\nu_H \frac{\partial U}{\partial x}\right) + \frac{\partial}{\partial y}\left(\nu_H \frac{\partial U}{\partial y}\right) \quad (1)$$

$$\frac{\partial V}{\partial t} + U\frac{\partial V}{\partial x} + V\frac{\partial V}{\partial y} = -g\frac{\partial \eta}{\partial y} + g\frac{V\left(U^2+V^2\right)^{1/2}}{C_b h} + \frac{\partial}{\partial x}\left(\nu_H \frac{\partial V}{\partial x}\right) + \frac{\partial}{\partial y}\left(\nu_H \frac{\partial V}{\partial y}\right) \quad (2)$$

$$\frac{\partial \eta}{\partial t} + \frac{\partial U}{\partial x} + \frac{\partial V}{\partial y} = 0 \quad (3)$$

where U and V are the velocities in the x and y directions, η is the elevation of the water surface, h is the water depth, C_b is the Chezy bed roughness, g is the gravity acceleration, and ν_H is the horizontal eddy viscosity.

The sediment-transport and morphology modules in Delft3D simulate bedload and suspended-load fluxes of cohesive and non-cohesive sediments and the exchange of sediment between the bed and water column. The transport of each sediment class is calculated separately, taking into account the availability of each fraction in the bed. Bedload sediment transport for non-cohesive sediment is computed with the formula of van Rijn (1993) (see supplemental material). Erosion and deposition shear stresses for sediment resuspension are based on the Shields parameter, while suspended load transport is calculated by solving the advection-diffusion equation:

$$\frac{\partial c}{\partial t} + U\frac{\partial c}{\partial x} + V\frac{\partial c}{\partial y} = \frac{\partial}{\partial x}\left(\varepsilon_s \frac{\partial c}{\partial x}\right) + \frac{\partial}{\partial y}\left(\varepsilon_s \frac{\partial c}{\partial y}\right) + \frac{c_{eq}-c}{T_s} \quad (4)$$

where c is the suspended sediment mass concentration, ε_s is the sediment eddy diffusivity, T_S is an adaptation time scale, and c_{eq} is the local equilibrium depth-averaged suspended sediment concentration. For cohesive sediments, the Partheniades–Krone formulations for erosion and deposition are used (Partheniades, 1965). In these formulations, the critical shear stress for erosion is always greater than or equal to the one for deposition; therefore, intermediate shear-stress conditions may exist for which neither erosion nor deposition occurs (see Delft3D manual for full reference).

Sediment resuspension in the bays of the VCR is governed by wind waves (Lawson et al. 2007; Mariotti et al. 2010). Our study applies the SWAN model with Delft3D to simulate wind waves under annual averaged wind speeds (Fig. 1). In the SWAN model, wind waves are described with the wave action density spectrum in the two-dimensional geographic space (Booij et al., 1999). The model accounts for wave generation, dissipation (whitecapping, bottom friction, and depth-induced breaking), and nonlinear wave-wave interactions. For computational reasons, the model is set up on the same square grid as the Delft3D model, with a 250 m cell size. Water level is set by the tidal cycle based on the studied tide and measurements at Hog Island NOAA station, Virginia, USA. The steady wave field is computed from the two more frequent annual wind speeds and directions neglecting coupling with currents: 1) 5 m s^{-1} from S-SSW; 2) 4 m s^{-1} from NE (wind data and statistics from Wachapreague NOAA station, Virginia, USA; tidesandcurrents.noaa.gov).

2.3 Effect of vegetation on flow

The Delft3D model allows users to specify bed roughness and flow resistance on a sub-grid level by defining various land use or roughness classes. One way to model vegetation in Delft3D is to correct the bed roughness using the equation proposed by Baptist (2005). Baptist's

formulation is based on the concept that vegetation can be modeled as rigid cylinders characterized by height h_v, density m, stems diameter D, and drag coefficient C_D. Various combinations of vegetation parameters can represent diverse wetland configurations under different water flow conditions. In this formulation, the velocity profile is divided in two flow zones: 1) a zone of constant flow velocity, u_v, inside the vegetated part and 2) a logarithmic velocity profile, u_u, above the vegetation starting from the velocity value u_v at the vegetation interface (Fig. 2). For the emergent vegetation this reduces to one flow zone with velocity u_v throughout the vegetation (Fig. 2A).

For the case of fully submerged vegetation (Fig. 2B), the total shear stress, τ_t is given as:

$$\tau_t = \rho g h i = \tau_b + \tau_v \tag{5}$$

where ρ is the water density, g is the gravity acceleration, i is the slope of the water surface, h is the water depth. τ_t is equal to the sum of the bed shear stress, τ_b, and the shear stress due to the vegetation drag, τ_v:

$$\tau_b = \frac{\rho g}{C_b^2} u_v^2 \tag{6}$$

$$\tau_v = \frac{1}{2} \rho C_D n h_v u_v^2 \tag{7}$$

where C_b is the Chézy bed roughness, C_D is the drag coefficient of the single vegetation stem, $n = m D$ is the vegetation density, h_v is the vegetation height, m is the number of stems per unit area, and D is the diameter of cylinders.

By Replacing τ_b and τ_v in Eq. (5) with the expressions given in (6) and (7), it is possible to calculate the uniform water flow velocity from the momentum balance equation as:

$$u_v = \sqrt{\frac{hi}{C_b^{-2}+(2g)^{-1}C_D n h_v}} \tag{8}$$

Combining Eq. 6 and Eq. 8 yields an expression for the vegetated bed shear stress, τ_{bv}, as a function of a reduction factor, f_s, times the total shear stress τ_t for the uniform flow velocity through the vegetation:

$$\tau_{bv} = f_s \tau_t, \quad f_s = \frac{1}{1+\frac{C_D n h_v C_b^2}{2g}} \tag{9a,b}$$

The Chézy friction value for totally submerged vegetation, C_{rs}, is defined as:

$$C_{rs} = \frac{\bar{u}}{\sqrt{hi}} \tag{10}$$

where $\bar{u}$ is the depth-averaged flow velocity. Introducing Eq. 5 and Eq. 10 in Eq. 9a, one can obtain the expression:

$$\tau_{bv} = f_s \frac{\rho g}{C_{rs}^2} \bar{u}^2 \tag{11}$$

where C_{rs} is defined as (see details in Baptist, 2005):

$$C_{rs} = \sqrt{\frac{1}{C_b^{-2}+(2g)^{-1}C_D n h_v}} + \frac{\sqrt{g}}{k} ln\left(\frac{h}{h_v}\right) \tag{12}$$

where k is the Von Karman constant ($k = 0.4$).

In the case of partially submerged vegetation (Fig. 2A), following the same procedure for fully submerged vegetation with total shear stress being the sum of bed shear stress, τ_b, and the shear stress due to the vegetation drag, τ_v (Eq. 5), we obtain:

$$ghi = \left(\frac{1}{2} C_D n h + \frac{g}{C_b^2}\right) u_v^2 \tag{13}$$

The flow velocity within the vegetation is:

$$u_v = \sqrt{\frac{hi}{C_b^{-2}+(2g)^{-1}C_D nh}} \tag{14}$$

which is equal to the depth-averaged velocity, $\bar{u}$, for emergent vegetation. Combining Eq. 6 and Eq. 14, the bed shear stress due to the flow velocity through the vegetation, $\tau_{bv,ns}$, becomes:

$$\tau_{bv,ns} = f_{ns}\tau_t, \quad f_{ns} = \frac{1}{1+\frac{C_D nhC_b^2}{2g}} \tag{15a,b}$$

The main difference between the two cases of submerged and emergent vegetation is in the reduction factor which in the first case includes the vegetation height, h_v (Eq. 9b), while in the second case contains the water depth, h (Eq. 15b).

The representative Chézy value for non-submerged vegetation is defined by:

$$C_r = \frac{u_v}{\sqrt{hi}} \tag{16}$$

Introducing Eq.8 in Eq. 16 the Chézy roughness coefficient for non-submerged vegetation becomes:

$$C_r = \sqrt{\frac{1}{C_b^{-2}+(2g)^{-1}C_D nh_v}} \tag{17}$$

Therefore in Eq. 12 the first term on the right-hand side equals the representative roughness for the partially submerged vegetation if $h = h_v$. Moreover, the value of C_{rs} is higher than the value of C_r leading to a smaller resistance for fully submerged vegetation. In our formulation, we do not account for capture of sediment particles by plant stems (Mudd et al., 2010).

2.5 Setup of hydrodynamic model

We simulate water flow and sediment transport on a computational grid of 150 by 459 cells, each 250 by 250 m in size (Fig. 1B). To set up, test, and validate our modelling framework,

we used extensive datasets collected in the VCR and available through the VCR-LTER portal (http://www.vcrlter.virginia.edu). The data encompass long-term measurements of sediment transport, salt marsh accretion, and vegetation characteristics within the salt marshes.

The VCR topography and bathymetry were extracted from existing Digital Elevation Models (e.g., Oertel et al., 2000; Richardson et al., 2014) and grids used in previous modeling studies (e.g., Mariotti et al., 2010; Safak et al., 2015; Wiberg et al., 2015). Where these detailed data sources did not provide coverage or good data quality, the bathymetry was based on local surveys and on NOAA charts (Mariotti et al., 2010; Safak et al., 2015). Depths outside the VCR were gathered from NOAA charts and datasets. The compiled dataset was interpolated, where necessary, to ensure that the main channels connecting the bays within the system were represented. Initial test runs showed that the dimensions of the swath of ocean included at the right boundary do not alter the numerical results. The simulated tide along the three open boundaries (North, East and South: Fig. 1B) is obtained by superimposing the various tidal harmonics with their corresponding phases and amplitudes (Fig. 4), recorded from the NOAA station (WAHV2, station ID: 8631044) in Wachapreague (VA) and VCR97053 in Hog Island (VA). A no flow condition is imposed at the landward boundaries.

Five meters of mixed non-cohesive and cohesive sediments are initially available for erosion at the bottom of the domain. The suspended sediment eddy diffusivities are calculated using horizontal large-eddy simulations and grain settling velocity (see Delft3D manual for full reference, https://oss.deltares.nl/web/delft3d/manuals). The horizontal eddy-viscosity coefficient is computed from a horizontal large-eddy simulation, and the background horizontal viscosity here set equal to 1 $m^2\ s^{-1}$. Bed roughness is set to a spatially and temporally constant Chézy value of 65 $m^{1/2}s^{-1}$. A time step of 60 s is adopted to satisfy all stability criteria.

Starting from an initial uniform sediment distribution in the bay domain, we allowed the bay area to evolve under continuous tidal cycles until it reached a steady state for the non-cohesive sediments (D_{50}= 125 μm; sediment density: ρ = 2,650 kg/m^3; dry bed density:ρ_d = 800 kg/m^3) and the two classes of cohesive sediment: D_{50}= 20 μm (settling velocity: w_s= 0.001 mm/s) and D_{50}= 63 μm (settling velocity: w_s= 3.0 mm/s). We defined this state as the point at which the suspended sediment concentration was stable in time.

The second part of our modeling experiments was to add two species of vegetation (*Spartina alterniflora* and *Zostera marina*) to the VCR bay (Fig. 3), based on orthophotogrammetry and field data (aerial photographs courtesy of Google Earth; Apollone, 2000). Within each vegetation community, vegetation characteristics were assumed to be uniform, with a given height, density, and stem diameter consistent with measurements acquired within *Spartina alterniflora* and *Zostera marina* communities (McGlathery et al., 2001). Five different spatial configurations for the vegetation communities were run (Fig. 3, Table 1). These scenarios were subjected to the same tidal forcing using main tidal harmonics (Fig. 4) to evaluate how vegetation affects sediment transport. Our vegetation experiments were designed to assess how vegetation impacts the hydrodynamics, sediment distribution and deposition in the VCR bays.

Model Runs	h_v (m)	n (m^{-1})	N_c (-)	V_v (-)
Seagrass	0.3 – 0.6	4 – 8	411	493.2 – 1,972.8
Salt marsh	0.7 – 1.4	2 – 4	2,361	3,305.4 – 13,221.6
Salt marsh + Seagrass	0.7 –1.4 0.3 – 0.6	2 – 4 4 – 8	2,772	3,798.6 (3,305.4 + 493.2) 15,194.4 (13,221.6 + 1972.8)
Seagrass 2x	0.3 – 0.6	4 – 8	822	986.4 – 3,945.6
Salt marsh + Seagrass 2x	0.7 –1.4 0.3 – 0.6	2 – 4 4 – 8	3,183	4,291.8 (3,305.4 + 986.4) 17,167.2 (13,221.6 + 3,945.6)
Seagrass 3x	0.3 – 0.6	4 – 8	1,233	1,479.6 – 5,918.4
Salt marsh + Seagrass 3x	0.7 –1.4 0.3 – 0.6	2 – 4 4 – 8	3,594	4,785.0 (3,305.4 + 1,479.6) 19,140.0 (13,221.6 + 5,918.4)

Table 1. Model runs and vegetation variables setup. V_v values are obtained from the product of N_c with both minimum and maximum values of h_v and n respectively. N_c for the salt marsh study is accounting for all the flooded cells populated with salt marsh vegetation during high tide.

To compare different runs with multiple vegetation species, we define a non-dimensional vegetation volume, V_v, as:

$$V_v = n\, h_v\, N_c \tag{18}$$

where N_c is the number of cells of vegetation flooded at high tide. To decouple the action of vegetative species on water and sediment fluxes, we computed a control run without vegetation.

Model outputs of interest included the maximum water volume contained in the bays during the tidal cycle highlighted in Figure 4A, the average sediment concentration, and the input and output of water and sediment. This approach offers the possibility to analyze large-scale flow and transport patterns and by plotting time series of fluxes within the VCR. Results are expected to be broadly representative of tidally dominated shallow estuaries with wind waves, in which along-shore currents, river discharge and other coastal processes are negligible, as are common along low-energy coastlines.

3. Results

3.1 Effect of currents and waves on bed shear stresses

Applying the Delft3D model, we calculated the maximum shear stress at each bay location during a spring tidal cycle (Fig. 4A). Strong tidal currents are sweeping the bottom near inlets (Fig. 4B, C, D) and are concentrated in the deep channels traversing the bays. The modeling effort showed a gradient in bottom shear stress in the east-west direction, with highest shear stresses in the eastern parts of the bays.

Waves and related bottom shear stresses were computed with a weighted average considering the two main wind directions, frequencies, and magnitudes (Fig. 5, 6). Because of the sheltering effect of the barrier islands, waves are locally generated and therefore have short periods on the order of 2-3 s. Results are shown for conditions when dominant wind directions are from south-southwest (Fig. 5) and northeast (Fig. 6). Wind waves are higher in the deeper, central parts of the bays (Fig. 5, 6). Bed shear stresses are larger near the tidal inlets because the interaction between tidal currents and wind waves. Fig. 5F and 6F shows the impact of seagrasses colonization on the reduction of significant wave height and bed shear stress.

The VCR bays are influenced by wind energy from the NE and SSW (Fagherazzi and Wiberg, 2009). Currents induced by these winds, in addition to tidal flows, are the major controls on bay sediment circulation, and the related ecological processes in the VCR (Wiberg et al., 2015). Here, we compare the effects of the two more frequent wind directions and speeds from SSW and NE with the case without winds but accounting for the tidal currents.

Northeasterly winds concentrate wave energy in the central parts of the bays (Fig. 5). SSW winds cause similar values of bed shear stress on tidal flats (Figure 6). An important difference between the two wind directions is noticeable in the bay channels. Interestingly, the presence of seagrass meadows has more of an effect on the flow rate when winds are from NE directions (Fig. 5), maybe due to the greater fetch for NE winds.

Maximum tidal current shear stresses decrease up to 5% when vegetation is present on the marsh platform (Fig. 7A). At the same time, bed shear stress decreases up to 1.5% in the channelized part of the bay.

3.2 Effect of vegetation on bay hydrodynamics

Our hydrodynamic results focus on a tidal cycle after the bay reaches a steady state. Model results show that vegetation produces a noteworthy reduction in the volume of water exchanged with the ocean (Fig. 7). In particular, the most vegetated study case exerted a reduction of up to 15% of the water volume exchanged in a tidal cycle relative to the case without vegetation. Because of their large expanse (Fig. 3), salt marshes have the greatest impact on the incoming volume of water, with an influence up to 5 times greater than that of seagrass beds (Fig. 7C).

Vegetation roughness also results in a redistribution of velocity in the system, slowing down the flow velocity in the marshes and slightly increasing the velocity at the tidal inlets because of topographic steering. In the most vegetated case (salt marsh and seagrass with density and vegetation height twice the values of the other runs), the averaged velocity of all tidal inlets is 2% higher than the case without vegetation (Fig. 7B). At the same time, the flow velocity decreases on the marshes and in the seagrass meadows, as showed by the shear stress ratio which decreases up to 5% (Fig. 7A). In addition, the model output suggests that the effects of higher velocity at the tidal inlets is related to deeper channels.

3.3 Effect of vegetation on sediment concentration.

Over a tidal cycle, the total amount of sediment in the water column is related to dilution, with peaks of suspended sediment during low tide and troughs during high tide (Fig. 8A). To track all sediment in the bay, our model computes the total amount of sediment in the defined bay and marsh platforms polygon. Total amount of sediment represents all deposited and suspended sediment in each cell inside the bay polygon. Vegetation have a marked effect on sediment trapped in the bays over a tidal cycle, with higher vegetation volume resulting in more sediment trapping (Fig. 8B). Addition of vegetation to the salt marsh induces the largest increase in sediment trapped and deposited in the entire bay, therefore less sediment is exiting through the

tidal inlets (Fig. 8). Doubling salt marsh and/or seagrass vegetation densities and heights results in a smaller increment of sediment deposition compared to the lower vegetation densities. In contrast, for low vegetation volumes, sediment concentrations in the bays and marshes are most sensitive to seagrass abundance (Fig. 8B), with the highest sediment concentrations associated with the seagrass 3x run. As non-dimensional vegetation volume increases beyond 2000 in the model, it is the presence of both salt marsh vegetation and seagrass that results in the greatest sediment concentrations. Across all vegetation communities, increasing vegetation volume is associated with monotonic increases in the amount of available sediment in the bay.

To differentiate among suspended and deposited sediment, we run the Delft3D morphological module until the model reaches an equilibrium concentration of suspended sediment. At that point, we compute sediment deposition and suspension. Higher values of vegetation volume in the bays decrease suspended sediment concentration but increase sediment deposition. Wind-generated waves clearly favor sediment resuspension in the bays leading to lower values of sediment deposition if compared with the tidal currents case (Fig. 8C).

4 Discussion

Our study reveals the important role that vegetation plays in altering hydrodynamics and sediment dynamics in the bays. In the physical approach used, spatial scales play an important role. While impacts of vegetation on sediment distribution are well understood at the patch scale (Carr et al., 2016), a general understanding at the bay scale is missing.

One of the most important results is that vegetation increases sedimentation and reduces sediment concentration in the water column (Fig. 8C), often a desirable outcome for the management of coastal barrier island complexes. A decrease in sediment concentration could be

beneficial for fisheries and oyster farming (Coco et al., 2006; Soletchnik et al., 2007). For example, Chesapeake Bay, USA, is characterized by high concentrations of suspended sediments which decrease water quality, directly inhibiting healthy oyster growth, and leading to fish mortality (Hardaway et al. 2000).

Another important implication is that, with increasing vegetation, velocity at the tidal inlets increases. This could potentially result in deeper channels and improved navigability through the inlets, but the limited increment (less than 2%) has likely a negligible effect. Previous works by Hubbard et al., 1979 showed how sediment distribution and channel morphology of tidal inlets are related to tidal hydrodynamics, while other modeling studies highlighted the impacts of tidal currents on the tidal inlet morphology (Dissanayake et al., 2009).

In scenarios with increased marsh vegetation, water exchange with the ocean is reduced, which could lead to higher nutrients retention and a risk of eutrophication. This effect is due to higher friction in the presence of vegetation, which reduces tidal propagation thus delaying the release of water (Fig. 7C). Wind-generated waves are the primary driving process affecting bottom shear stresses (Fig. 5 and 6). However, the impact of tidal currents on seagrass platforms is marked and evident in figure 4. In particular, if seagrasses colonize parts of the bay, significant wave height and bed shear stress are low because of the dissipation caused by submerged vegetation (Fig 5F and 6F).

The hydraulic roughness due to vegetation is modeled in a variety of ways in Delft3D, including the equations proposed by Baptist (2005). The Baptist equation was developed assuming rigid vegetation, which is essentially true in salt marshes dominated by *Spartina alterniflora*. In contrast, the seagrass found in the VCR, *Zostera marina*, is flexible and the Baptist model may over-estimate its roughness. Baptist's equation has been widely tested with

field data and through laboratory experiments with natural and artificial vegetation (Arboleda et al., 2010). In addition, many experiments have compared the predicted results with experimental data, finding a good fit (Crosato and Saleh, 2010; Arboleda et al., 2010). Crosato and Saleh (2010) provide another validation of the Baptist's equation on the effects of floodplain vegetation on river planform.

Our results can be used to inform an understanding of morphodynamic processes over longer time scales, through consideration of the seasonal effects of vegetation on suspended sediment concentrations. During the growing season (May - August), expansion of vegetation biomass decreases suspended sediment concentration (Fig. 8C) in the bay as a result of higher bottom roughness. Nardin and Edmonds (2014) show how important vegetation stage is during river flood events in deltas. Because the tide is periodic and independent of seasons while vegetation seasonally changes, the bays show an increased retention of sediment during summer when the vegetation reaches the highest biomass (Fig. 8C).

Our research shows that salt marshes alone influence sediment retention in the bays more than seagrass beds. However, seagrasses colonize parts of the bays too deep to support salt marsh vegetation, and therefore constitute an important net addition to sediment retention. In summary, even if it is less effective at trapping sediments in the bays, seagrass meadows play a central role in an environment where salt marsh grasses cannot survive.

The presented study agrees with previous study of Novacky et al., (2017) in Chincoteague Bay, U.S.A, which shows through field observations a wave-height reduction and wave-energy dissipation into the seagrass meadow. In agreement with our results, Novacky et al., (2017) reveals that vegetation was the most significant component of wave dissipation at the study site.

Our study highlights the double benefits of seagrass as a supporter of salt marsh in enhancing bays resilience. On the one hand, seagrass helps the salt marsh to survive during storms by reducing wave energy; on the other hand, seagrass generates more friction in subtidal parts of the bay where salt marsh cannot survive, thereby trapping more sediment.

5. Conclusions

Our numerical results show that salt marshes and seagrass beds reduce up to 15% the volume of water exchanged in a tidal cycle in a shallow coastal bay. Vegetation affects bay geomorphology by locally reducing bed shear stress and hence increasing sediment deposition. We study alternative densities, heights and spatial distributions of seagrass and salt marsh grasses; presented results can thus inform the design of restoration strategies in shallow coastal bays, such as the Virginia Coast Reserve. The proposed study highlights the role of seagrass as an ally of salt marsh vegetation in generating bay resiliency. In fact, seagrasses enhance sediment deposition and generate more friction in a part of the bay where salt marsh plants cannot survive.

References

Apollone, E., Organic matter distribution and turnover along a gradient from forest to tidal creek. Master thesis, Department of Biology, East Carolina University, 2000.

Arboleda AM, Crosato A, Middelkoop H. Reconstructing the early 19th-century Waal River by means of a 2D physics-based numerical model. Hydrol. Process. 2010;24: 3661‐75. http://dx.doi.org/10.1002/hyp.7804.

Baptist, M. Modelling floodplain biogeomorphology Ph.D. thesis, Delft University of Technology, ISBN 90-407-2582-9. (2005).

Baptist MJ, Babovic V, Rodríguez Uthurburu J, Keijzer M, Uittenbogaard RE, Mynett A, Verwey A. 2007. On inducing equations for vegetation resistance. Journal of Hydraulic Research 45(4): 435–450.

Boesch, D. F. 2006. Scientific requirements for ecosystem-based management in the restoration of Chesapeake Bay and Coastal Louisiana. *Ecological Engineering* 26:6–26.

Booij, N., Ris, R.C., Holthuijsen, L.H., 1999. A third-generation wave model for coastal regions, Part I, model description and validation. Journal of Geophysical Research 104, 7649–7666.

Carr J, D'Odorico P, McGlathery KJ, Wiberg PL (2010) Stability and bistability of seagrass ecosystems in shallow coastal lagoons:role of feedbacks with sediment re - suspension and light attenuation. J Geophys Res 115: G03011 doi: 10.1029/2009JG001103

Carr, J.A., D'Odorico, P., McGlathery, K.J. and Wiberg, P.L., 2016. Spatially explicit feedbacks between seagrass meadow structure, sediment and light: Habitat suitability for seagrass growth. Advances in Water Resources, 93, pp.315-325.

Collins, D. B. G., R. L. Bras, and G. E. Tucker. 2004. Modeling the effects of vegetation-erosion coupling on landscape evolution. Journal of Geophysical Research: Earth Surface (2003–2012) 109.

Coco, G., F.T. Simson, M.O. Green, and J.E. Hewitt. 2006. Feedbacks between Bivalve Density, Flow, and Suspended Sediment Concentration on Patch Stable States. Ecology 87: 2862-2870.

Crosato, A. and Saleh, M. S. (2011), Numerical study on the effects of floodplain vegetation on river planform style. Earth Surf. Process. Landforms, 36: 711–720. doi:10.1002/esp.2088.

Cucco, A., Umgiesser, G., 2006. Modeling the Venice Lagoon residence time. Ecol. Model. 193, 34–51.

Dai, Z. J., S. Fagherazzi, X. F. Mei, and J. J. Gao (2016), Decline in suspended sediment concentration delivered by the Changjiang (Yangtze)River into the East China Sea between 1965 and 2013, Geomorpholo gy, 268, 123–132, doi:10.1016/j.geomorph.2016.06.009.

D'Alpaos, A., S. Lanzoni, M. Marani, and A. Rinaldo. 2007. Landscape evolution in tidal embayments: Modeling the interplay of erosion, sedimentation, and vegetation dynamics. Journal of Geophysical Research 112:F01008

Dissanayake, D. M. P. K., J. A. Roelvink, and M. Van der Wegen (2009), Modelled channel pattern in schematised tidal inlet, Coastal Eng., 56, 1069–1083.

Emory, K.O., Aubrey, D.G., 1991. Sea Levels, Land Levels and Tide Gauges. Springer Verlag, NY.

Fagherazzi, S., Marani, M. and Blum, L.K., 2004. *The ecogeomorphology of tidal marshes*. American Geophysical Union.

Fagherazzi, S., and P. L. Wiberg (2009), Importance of wind conditions, fetch, and water levels on wave generated shear stresses in a shallow intertidal basin, J. Geophys. Res., 114, F03022, doi:10.1029/ 2008JF001139.

Fagherazzi, S., Kirwan, M.L., Mudd, S.M., Guntenspergen, G.R., Temmerman, S., D'Alpaos, A., Koppel, J., Rybczyk, J.M., Reyes, E., Craft, C. and Clough, J., 2012. Numerical models of salt marsh evolution: Ecological, geomorphic, and climatic factors. *Reviews of Geophysics*, 50(1).

Folmer, E. O., van der Geest, M., Jansen, E., Olff, H., Anderson, T. M., Piersma, T., & van Gils, J. A. (2012). Seagrass–sediment feedback: an exploration using a non-recursive structural equation model. Ecosystems, 15(8), 1380-1393.

Fugate, D.C., Friedrichs, C.T., Bilgili, A., 2006. Estimation of residence time in a shallow back barrier lagoon, Hog Island Bay, Virginia, USA. In: Spaulding, M. (Ed.), 9th International Conference on Estuarine and Coastal Modeling, Charleston, SC

Gurnell, A. M., J. M. O'Hare, M. T. O'Hare, M. J. Dunbar, and P. M. Scarlett (2010), An exploration of associations between assemblages of aquatic plant morphotypes and channel geomorphological properties within British rivers, Geomorphology, 116(1–2), 135–144, doi:10.1016/j.geomorph.2009.10.014.

Hagy J.D., W.R. Boynton, C.W. Keefe, K.V. Wood. Hypoxia in Chesapeake Bay, 1950–2001: Long-term change in relation to nutrient loading and river flow. Estuaries, 27 (2004), pp. 634-658

Hardaway, C.S., Milligan, D.A., Brinkdley R., and Hobbs C.H. 2000. Maryland Delaware Shoreline: Long Term Trends versus Short term Variability. In Hobbs, C.H. Environmental

survey of Potential Sand Resource Sites Offshore Delaware and Maryland, Final Project Report. Virginia Institute of Marine Science, Gloucester Point, VA.

Hubbard, D.K., Oertel, G., and Nummedal, D., 1979. The role of waves and tidal currents in the development of tidal-inlet sedimentary structures and sand body geometry: examples from North Carolina, South Carolina and Georgia. J. Sed. Petrol.,49, 1073 – 1092.

Kemp W.M., R. Batiuk, R. Bartleson, P. Bergstrom, V. Carter, C. Gallegos, W.Hunley, L. Karrh, E. Koch, J. Landwehr, K. Moore, L. Murray, M. Naylor, N. Rybicki, J.C.Stevenson, D. Wilcox. Habitat requirements for submerged aquatic vegetation in Chesapeake Bay: water quality, light regime, and physical-chemical factors, Estuaries, 27 (2004), pp. 363-37

Kemp W.M., W.R. Boynton, J.E. Adolf, D.F. Boesch, W.C. Boicourt, G. Brush, J.C.Cornwell, T.R. Fisher, P.M. Glibert, J.D. Hagy. Eutrophication of Chesapeake Bay: historical trends and ecological interactions. Marine Ecology Progress Series, 303 (2005), pp. 1-29.

Larsen, G. Laurel and Judson W. Harvey, "How Vegetation and Sediment Transport Feedbacks Drive Landscape Change in the Everglades and Wetlands Worldwide." The American Naturalist 176, no. 3 (September 2010): E66-E79.

Lawson, S. E., P. L. Wiberg, K. J. McGlathery, and D. C. Fugate (2007), Wind -driven sedime suspension controls light availability in a shallow coastal lagoon, Estuaries Coasts, 30(1), 102–112.

Lesser G, Roelvink J, Van Kester J, Stelling G. Development and validation of a three-dimensional morphological model. Coast Eng 2004; 51:883– 915.

Luhar, M., and H. M. Nepf. 2013. From the blade scale to the reach scale: A characterization of aquatic vegetative drag. Advances in Water Resources 51:305–316.

Marani, M., Da Lio, C. and D'Alpaos, A., 2013. Vegetation engineers marsh morphology through multiple competing stable states. Proceedings of the National Academy of Sciences, 110(9), pp.3259-3263.

Mariotti, G., Fagherazzi, S., Wiberg, P.L., McGlathery, K.J., Carniello, L., Defina, A., 2010. Influence of storm surges and sea level on shallow tidal basin erosive processes. J. Geophys. Res. 115 (C11012). http://dx.doi.org/10.1029/2009JC005892

McGlathery, K.J., Anderson, I.C., Tyler, A.C., 2001. Magnitude and variability of benthic and pelagic metabolism in a temperate coastal lagoon. Mar. Ecol. Prog. Ser. 216, 1–15

McGlathery, K.J., Sundback, K., Anderson, I.C., 2007. Eutrophication patterns in shallow coastal bays and lagoons: the role of plants in the coastal filter. Mar. Ecol. Prog. Ser. 348, 1–18

McGlathery KJ, Reynolds LK, Cole LW, Orth RJ, Marion SR, Schwarzschild A (2012) Recovery trajectories during state change from bare sediment to eelgrass dominance. Mar Ecol Prog Ser 448:209-221. https://doi-org.proxy-um.researchport.umd.edu/10.3354/meps0957

McLoughlin, S.M., Wiberg, P.L., Safak, I., McGlathery, K.J., (2015). Rates and forcing of marsh edge erosion in a shallow coastal bay, Estuaries and Coasts 38, 620-638. http://dx.doi.org/10.1007/s12237-014-9841-2.

Moore, K. A. (2004). Influence of seagrasses on water quality in shallow regions of the lower Chesapeake Bay. Journal of Coastal Research, 162-178.

Mudd, S. M., A. D'Alpaos, AND J. T. Morris. 2010. How does vegetation affect sedimentation on tidal marshes? Investigating particle capture and hydrodynamic controls on biologically mediated sedimentation. Journal of Geophysical Research: Earth Surface (2003–2012) 115.

Nardin, W., and Edmonds, D. A. (2014). Optimum vegetation height and density for inorganic sedimentation in deltaic marshes. Nature Geoscience, 7(10), 722-726, doi:10.1038/ngeo2233.

Nardin W., D. A. Edmonds and S. Fagherazzi, Influence of vegetation on spatial patterns of sediment deposition in deltaic islands during flood, Advances in Water Resources, 2016, doi:10.1016/j.advwatres.2016.01.001.

Newell, R. I., & Koch, E. W. (2004). Modeling seagrass density and distribution in response to changes in turbidity stemming from bivalve filtration and seagrass sediment stabilization. Estuaries, 27(5), 793-806.

Nowacki, DJ, A Beudin, NK Ganju, 2017. Spectral wave dissipation by submerged aquatic vegetation in a back barrier estuary. Limnology and Oceanography 62 (2), 736-753.

Oertel, G.F., Carlson, C., Overman, K., 2000. Bathymetry of Hog Island Bay, Virginia Coast Reserve Long-Term Ecological Research Project. Data Publication knblter-vcr.143.12.

Oertel, G.F., 2001. Hypsographic, hydro-hypsographic and hydrological analysis of coastal bay environments Great Machipongo Bay, Virginia. J. Coast. Res. 17 (4), 775–783.

Orth RJ, McGlathery KJ (2012) Eelgrass recovery in the coastal bays of the Virginia Coast Reserve, USA. Mar Ecol Prog Ser 448:173–176.

Partheniades, E., 1965. Erosion and deposition of cohesive soils. Am. Soc. Civil. Eng., J. Hydraul. Div., Proceed. 92, 79–81.

Richardson, D., J. Porter, G. Oertel, R. Zimmerman, C. Carlson, K. Overman. 2014. Integrated topography and bathymetry for the eastern shore of Virginia. Long Term Ecological Research Network. Available from http://dx.doi.org/10.6073.

van Rijn, L. C. (1993), Principles of Sediment Transport in Rivers, Estuaries, and Coastal Seas, edited, Aqua publications, Amsterdam.

Safak I., Wiberg P.L, Richardson D. L, Kurum M.O., 2015. Controls on residence time and exchange in a system of shallow coastal bays. Continental Shelf Research. 97(1) 7-20.

Sallenger, A., K. Doran, and P. Howd (2012), Hotspot of accelerated sea-level rise on the Atlantic coast of North America, Nat. Clim. Change, 2, 884–888, doi:10.1038/nclimate1597.

Soletchnik, P., M. Ropert, J. Mazurie, P. Gildas Fleury, and F. Le Coz. 2007. Relationships between oyster mortality patterns and environmental data from monitoring databases along the coasts of France. Aquaculture 271:384-400.

Temmerman, S., Meire, P., Bouma, T. J., Herman, P. M., Ysebaert, T., & De Vriend, H. J. (2013). Ecosystem-based coastal defence in the face of global change. Nature, 504(7478), 79-83.

Temmerman, S., Bouma, T.J., Govers, G., Wang, Z.B., De Vries, M.B. and Herman, P.M.J., 2005. Impact of vegetation on flow routing and sedimentation patterns: Three -dimensional modeling for a tidal marsh. Journal of Geophysical Research: Earth Surface, 110(F4).

Walters, D., L. J. Moore, O. D. Vinent, S. Fagherazzi, and G. Mariotti. 2014. Interactions between barrier islands and backbarrier marshes affect island system response to sea level rise: insights from a coupled model. J. Geophys. Res., series F 119:1–19.

Wiberg, P.L., J.A. Carr, I. Safak, A. Anutaliya, 2015. Quantifying the distribution and influence of non-uniform bed properties in shallow coastal bays. Limnology & Oceanography Methods 13: 746-762, doi: 10.1002/lom3.10063.

Figure captions

Figure 1. A) Study site: Virginia Coast Reserve (VA), located on the Delmarva Peninsula (red box) in the U.S. Mid-Atlantic coast. White dashed lines shows the numerical model domain while white lines highlight the cross sections used for quantifying water and sediment fluxes

(Aerial photographs courtesy of Google Earth, 2015). B) Computational domain with boundary conditions. Color map shows elevation extracted from existing Digital Elevation Models (e.g., Oertel et al., 2000; Mariotti et al., 2010) and grids used in previous modeling studies.

Figure 2. Schematization of the velocity profile in the Delft3D vegetation model. A) Vegetation partially submerged and B) fully submerged. Modified from Nardin and Edmonds (2014). C) Set up of modeled vegetative species distribution at VCR

Figure 3. Modeled vegetative species distribution at VCR in a Delft3D-SWAN model domain. Red and black dots show current distribution of salt marshes and seagrasses, respectively, in the bays. Areas contoured by blue dots indicate possible future seagrass expansion.

Figure 4. A) Water level simulated in the VCR estuary. Red box shows the focus interval used to present study's result. Maximum bed shear stress produced by tidal currents in the bays: B) no vegetation C) only salt marsh vegetation and D) salt marsh vegetation and current seagrass distribution. The velocity is computed utilizing a sinusoidal tide with amplitude equal to the great diurnal range (1.6 m). The rectangular inset is the VCR bathymetry. Green and red ellipses show where the vegetation effect is more pronounced.

Figure 5. A) Significant wave height for unvegetated bay conditions computed with the annual averaged wind speeds (5 m s^{-1}) and the wind main direction S-SSW; B) only salt marsh vegetation; C) current salt marsh and seagrass vegetation distribution. D) bed shear stresses calculated at mean water level in the unvegetated case, E) shear stresses with only salt marsh vegetation and F) shear stresses with salt marsh vegetation and current seagrass distribution. Inset in A) is the model domain and bathymetry. Green and red ellipses show where the vegetation effect is more pronounced (wind data and statistics from Wachapreague NOAA

station, Virginia, USA; tidesandcurrents.noaa.gov).

Figure 6. A) Significant wave height for unvegetated bay conditions computed with the annual averaged wind speeds (4 m s^{-1}) and the wind main direction NE; B) wave height with only salt marsh vegetation; and C) wave height with salt marsh vegetation and current seagrass distribution. D) bed shear stresses calculated at mean water level in the unvegetated case. E) shear stresses with only salt marsh vegetation and F) shear stresses with salt marsh vegetation and current seagrass distribution. Inset in A) is the model domain and bathymetry. Green and red ellipses show where the vegetation effect is more pronounced.

Figure 7. A) R_{SS} is the ratio between bottom shear stress in the vegetated case and the shear stress in the unvegetated case as a function of vegetation volume V_v. Colors show different conditions of tidal currents and waves. B) Averaged flow velocity U_{ch} in the tidal inlets as a function of non-dimensional volume of vegetation V_v. C) Water volume in the bays during a single tidal cycle. Colored and dashed lines display the total amount of water present in the bays as a function of vegetation characteristics.

Figure 8. A) Water levels and total sediment in the bay-polygon in two tidal cycles; B) Non-dimensional suspended sediment ratio, $R_S = R^v_S / R^{nv}_S$, as a function of vegetation volume. R^v_S is the averaged suspended sediment concentration in the vegetated case, while, R^{nv}_S is the averaged suspended sediment concentration without vegetation. Colored lines show different vegetation configurations. C) Non-dimensional suspended (from waves and tidal currents re-suspension), deposited, and total sediment ratios, R_s, as a function of vegetation volume.

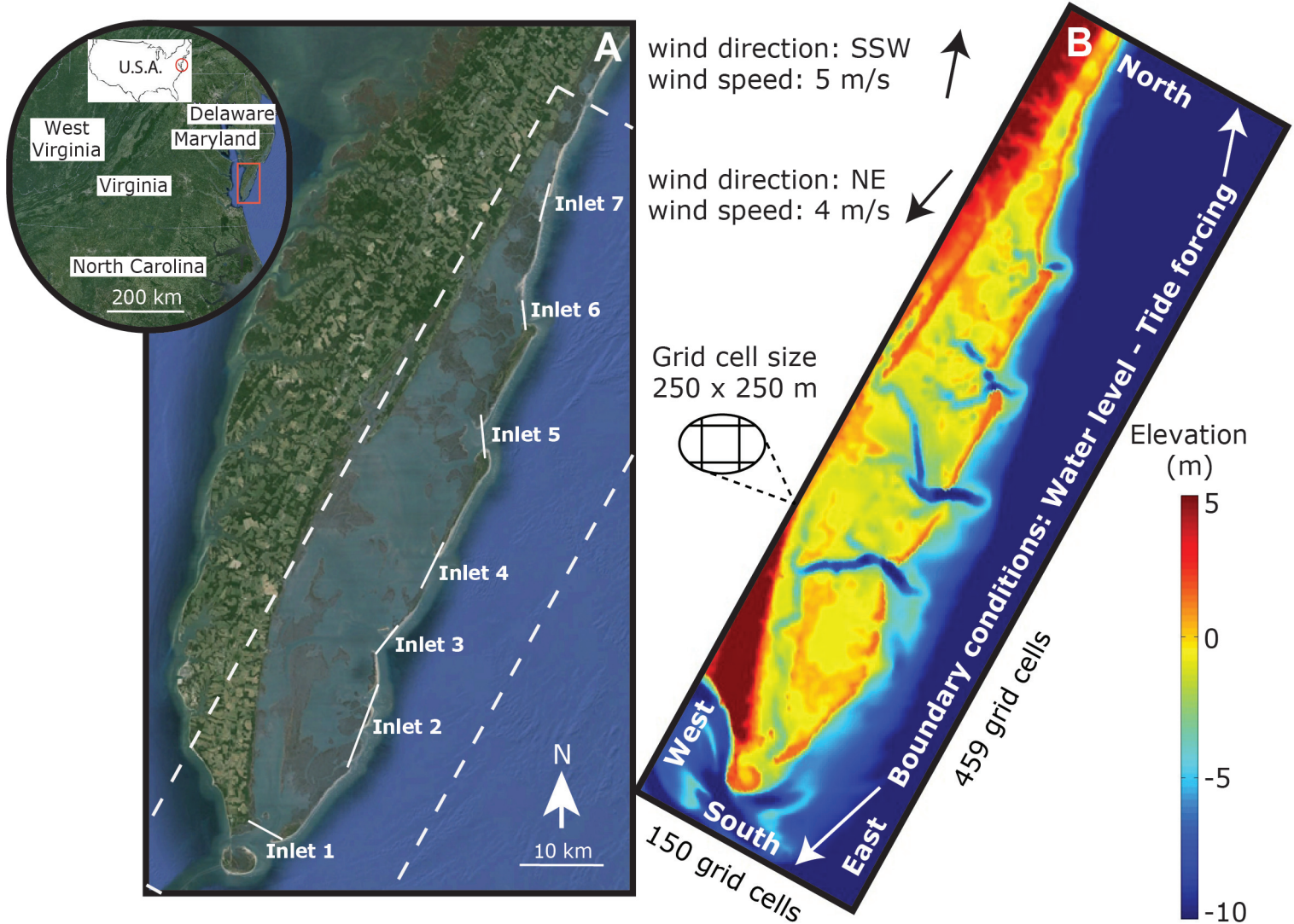
A
U.S.A.
West Virginia
Delaware
Maryland
Virginia
North Carolina
200 km
Inlet 7
Inlet 6
Inlet 5
Inlet 4
Inlet 3
Inlet 2
Inlet 1
N
10 km
wind direction: SSW
wind speed: 5 m/s
wind direction: NE
wind speed: 4 m/s
Grid cell size
250 x 250 m
B
North
West
South
East
Boundary conditions: Water level - Tide forcing
459 grid cells
150 grid cells
Elevation
(m)
5
0
-5
-10

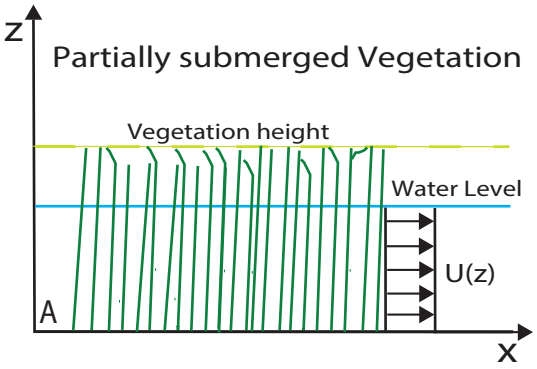
z
Partially submerged Vegetation
Vegetation height
Water Level
U(z)
A
x

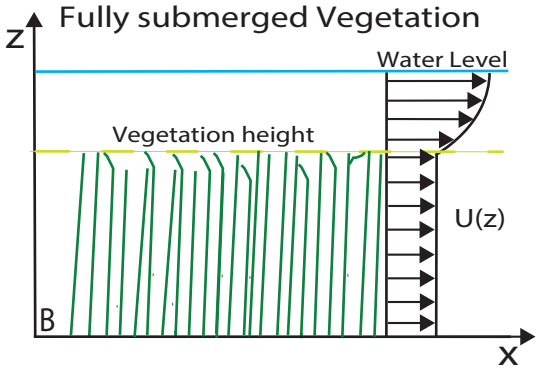
z
Fully submerged Vegetation
Water Level
Vegetation height
U(z)
B
x

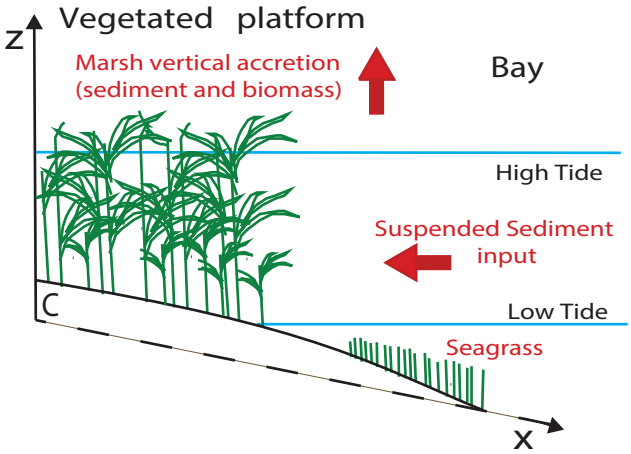
z
Vegetated platform
Marsh vertical accretion
(sediment and biomass)
Bay
High Tide
Suspended Sediment
input
Low Tide
C
Seagrass
x

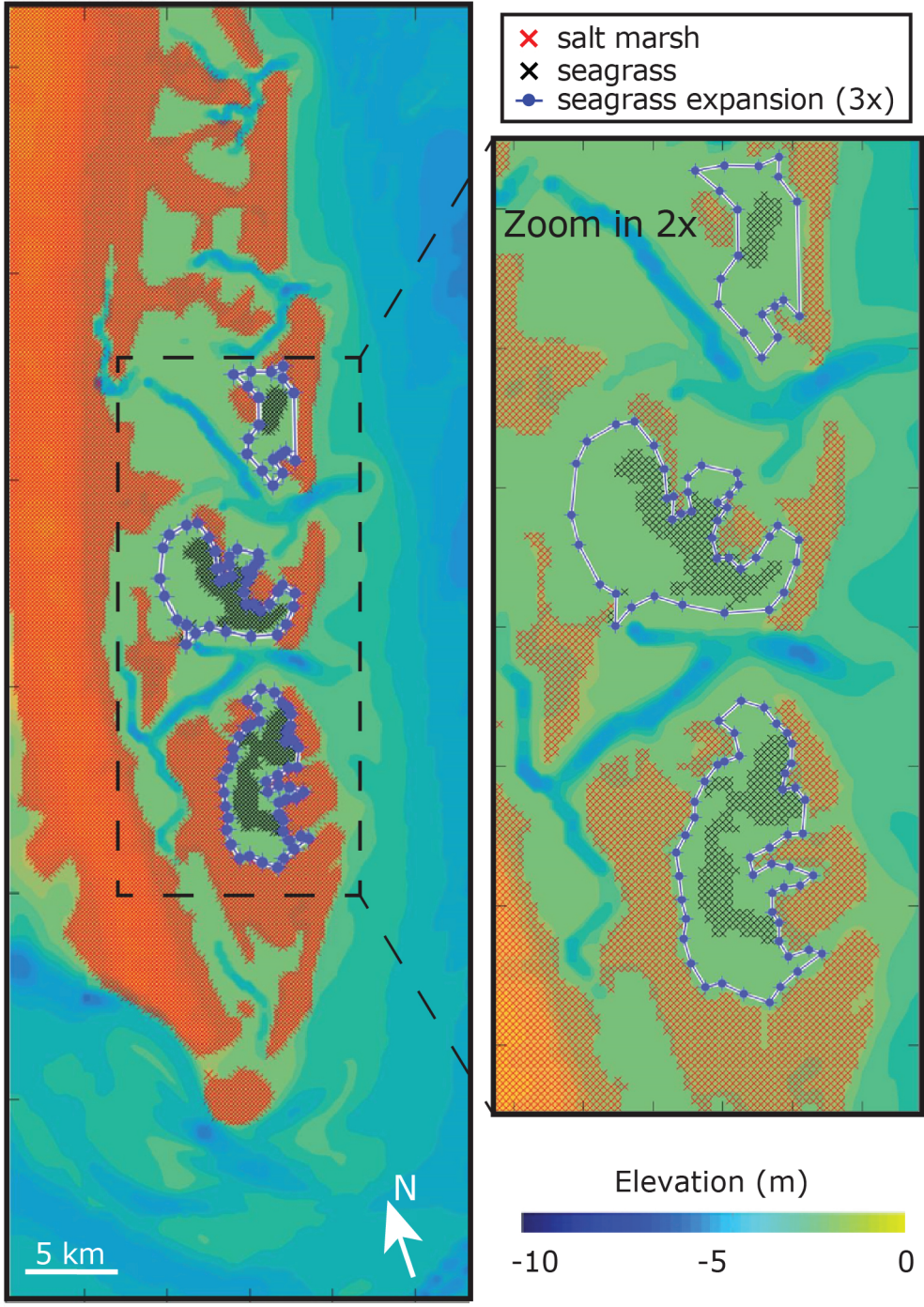
salt marsh
seagrass
seagrass expansion (3x)
Zoom in 2x
N
5 km
Elevation (m)
-10
-5
0

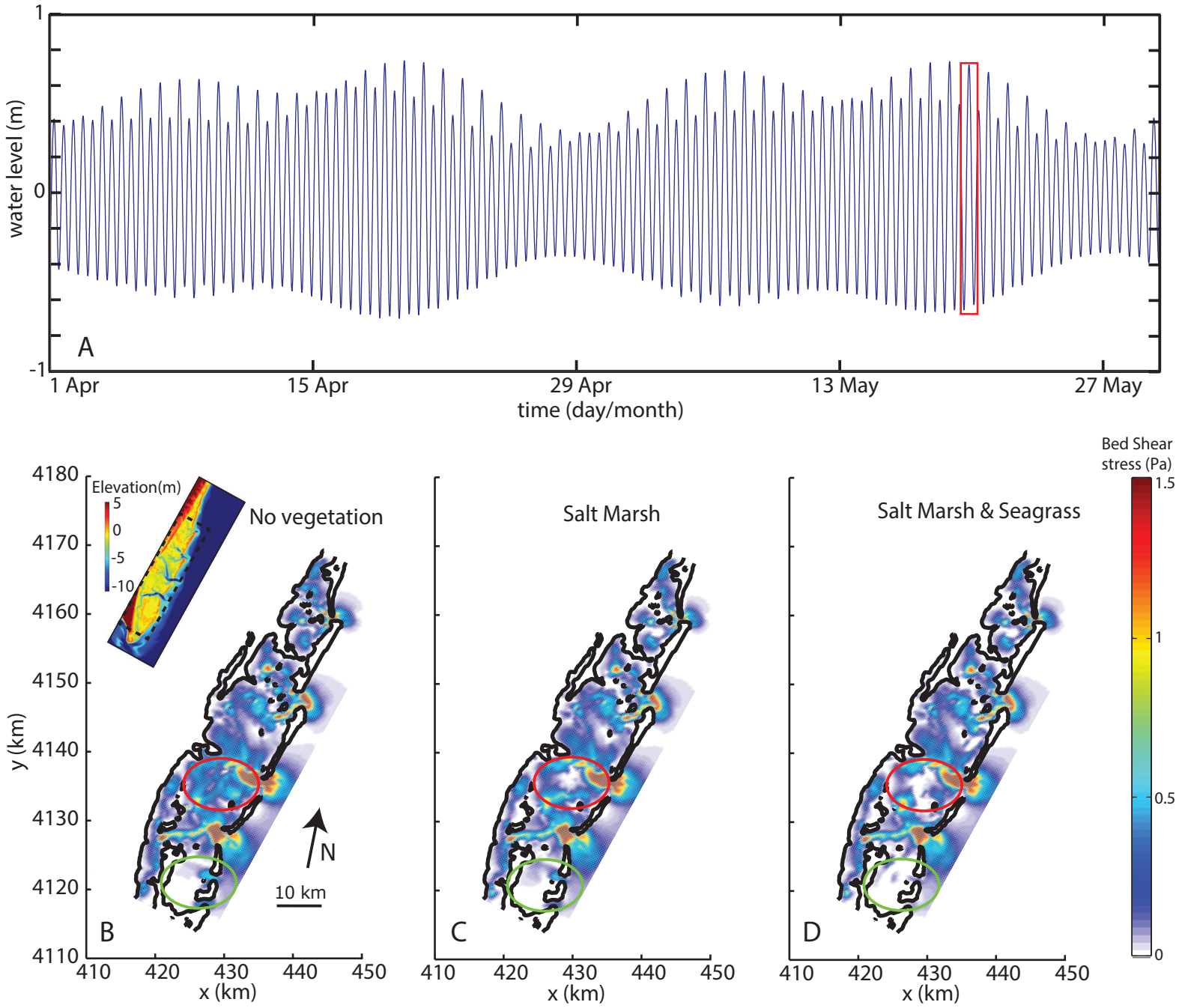
water level (m)
1
0
-1
A
1 Apr
15 Apr
29 Apr
13 May
27 May
time (day/month)
Elevation(m)
5
0
-5
-10
No vegetation
Salt Marsh
Salt Marsh & Seagrass
Bed Shear stress (Pa)
1.5
1
0.5
0
y (km)
4180
4170
4160
4150
4140
4130
4120
4110
410
420
430
440
450
x (km)
N
10 km
B
C
D

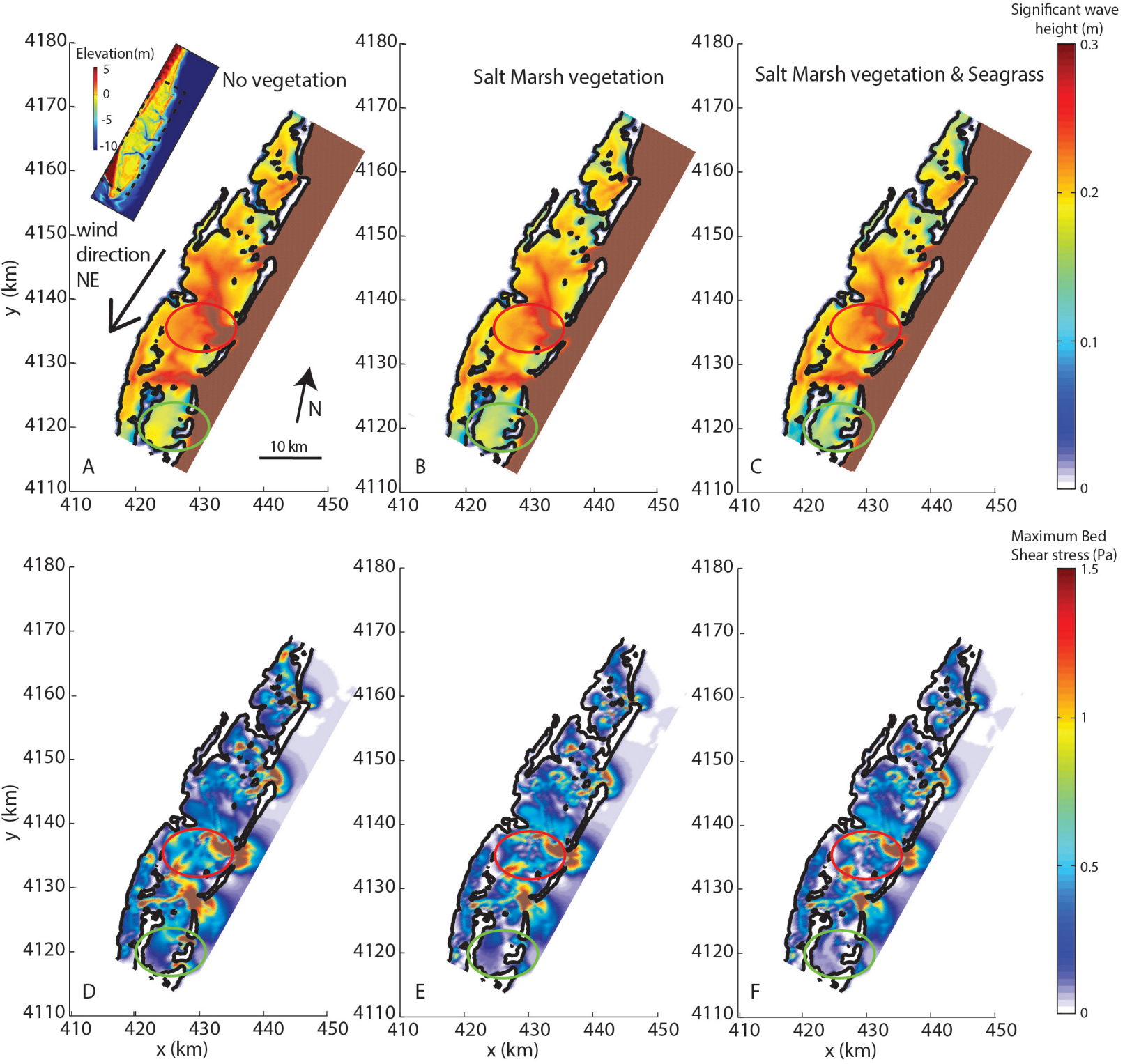
Significant wave height (m)
0.3
0.2
0.1
0
Elevation(m)
5
0
-5
-10
No vegetation
Salt Marsh vegetation
Salt Marsh vegetation & Seagrass
wind direction NE
N
10 km
A
B
C
D
E
F
y (km)
x (km)
4180
4170
4160
4150
4140
4130
4120
4110
410
420
430
440
450
Maximum Bed Shear stress (Pa)
1.5
1
0.5
0

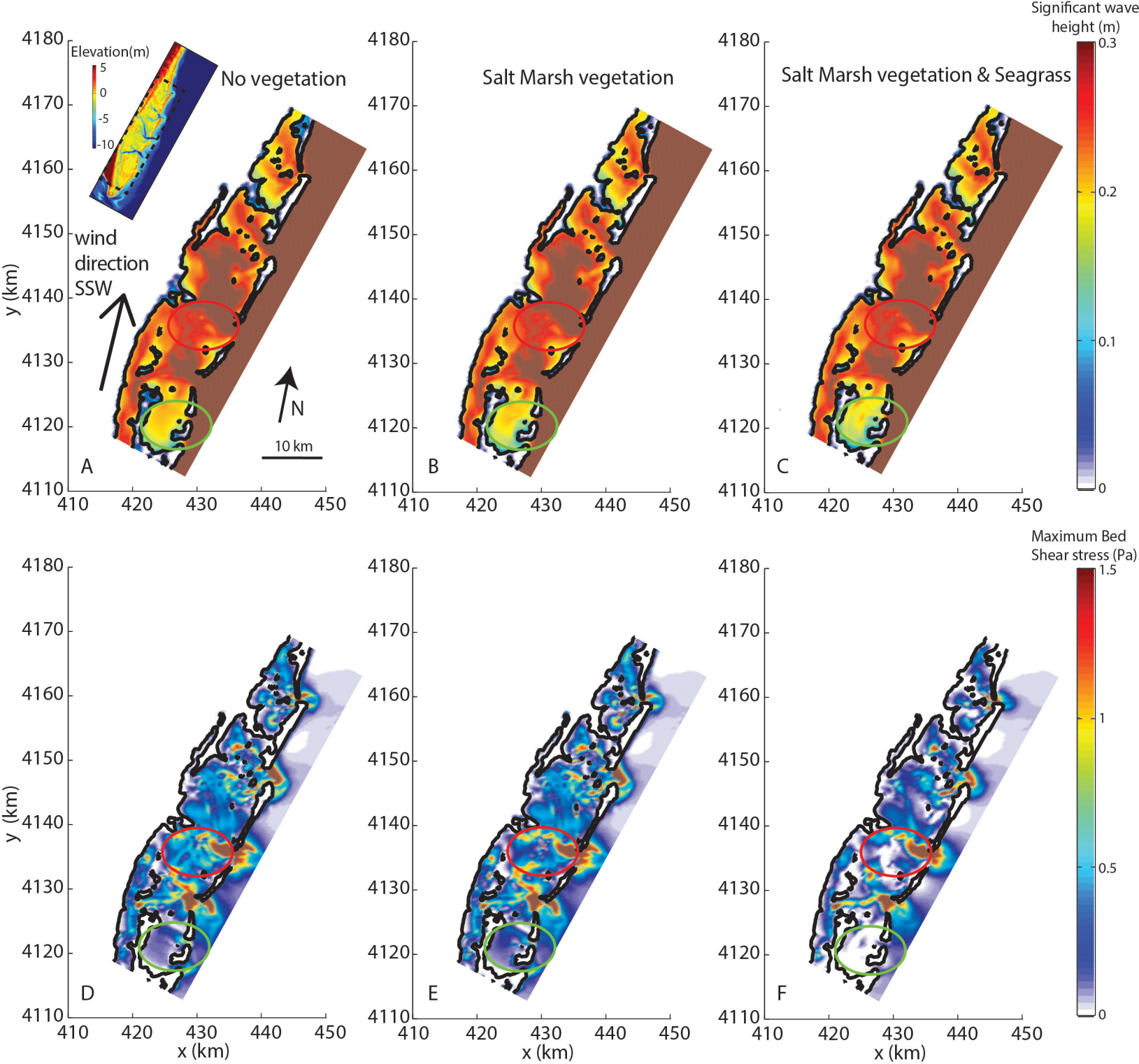
Elevation(m)
5
0
-5
-10
No vegetation
Salt Marsh vegetation
Salt Marsh vegetation & Seagrass
wind
direction
SSW
N
10 km
A
B
C
D
E
F
y (km)
x (km)
4180
4170
4160
4150
4140
4130
4120
4110
410
420
430
440
450
Significant wave
height (m)
0.3
0.2
0.1
0
Maximum Bed
Shear stress (Pa)
1.5
1
0.5
0

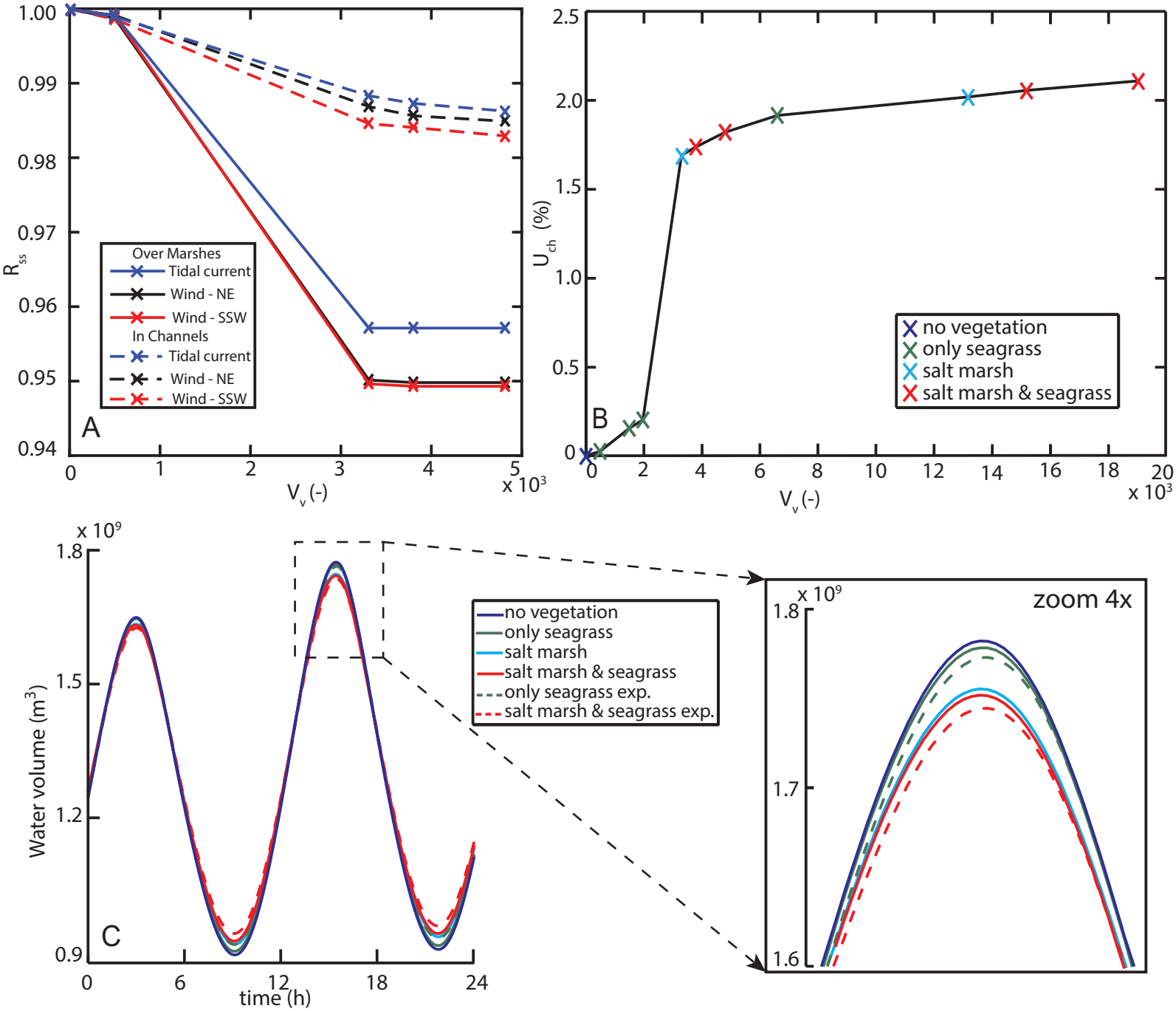
A
R_{ss}
V_v (-)
x 10^3
Over Marshes
Tidal current
Wind - NE
Wind - SSW
In Channels
Tidal current
Wind - NE
Wind - SSW
B
U_{ch} (%)
V_v (-)
x 10^3
no vegetation
only seagrass
salt marsh
salt marsh & seagrass
C
x 10^9
Water volume (m^3)
time (h)
no vegetation
only seagrass
salt marsh
salt marsh & seagrass
only seagrass exp.
salt marsh & seagrass exp.
zoom 4x
x 10^9

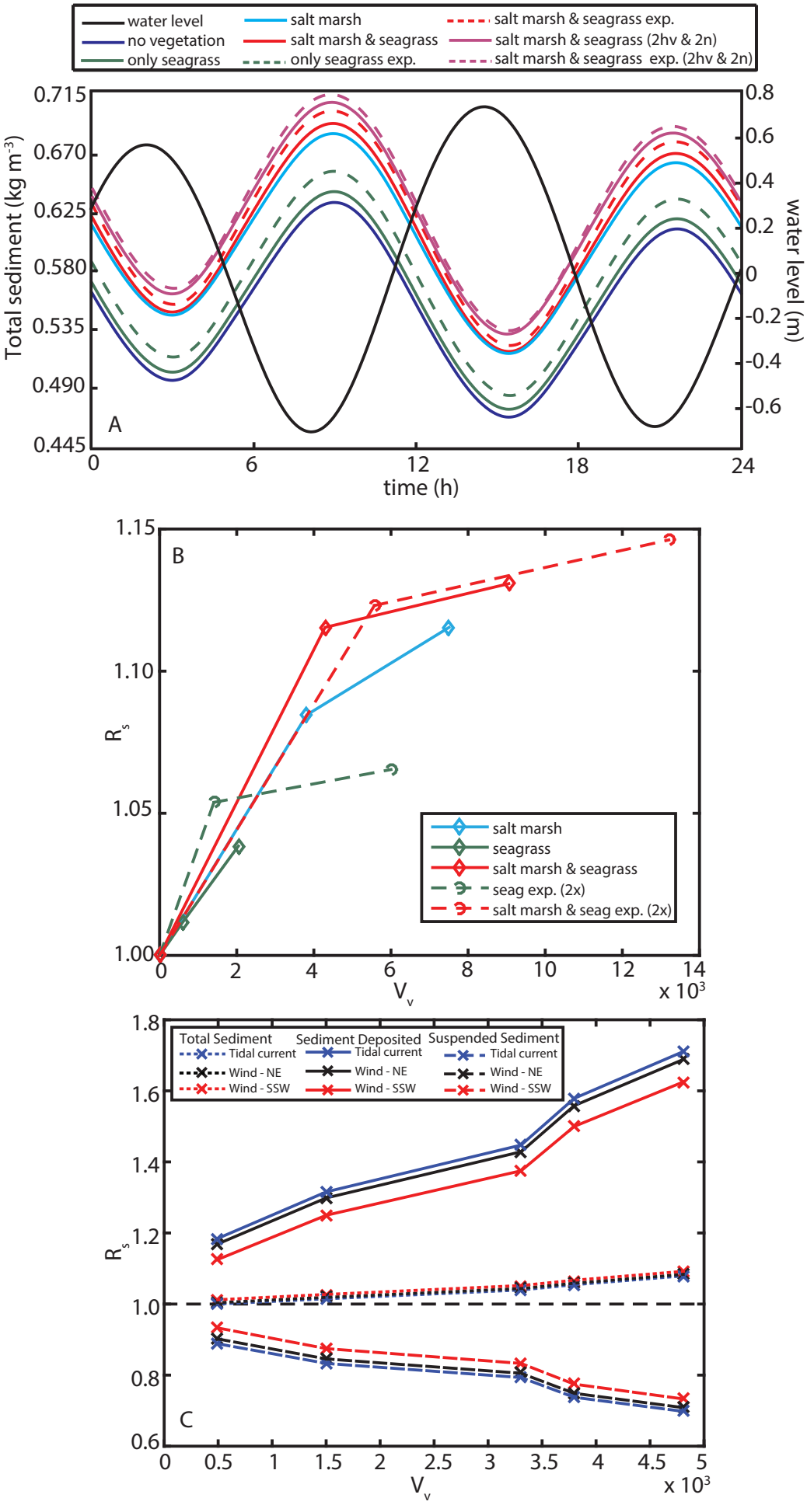
water level
no vegetation
only seagrass
salt marsh
salt marsh & seagrass
only seagrass exp.
salt marsh & seagrass exp.
salt marsh & seagrass (2hv & 2n)
salt marsh & seagrass exp. (2hv & 2n)
Total sediment (kg m-3)
water level (m)
time (h)
A
B
Rs
Vv
x 10^3
salt marsh
seagrass
salt marsh & seagrass
seag exp. (2x)
salt marsh & seag exp. (2x)
Total Sediment
Sediment Deposited
Suspended Sediment
Tidal current
Wind - NE
Wind - SSW
C